Bachelor Thesis

Exploration of an Origin of Anisotropy and its Effect upon Invariant Mass Reconstruction in a Two-Body Decay

Van Swinderen Institute
for Particle Physics and Gravity
Rijksuniversiteit Groningen

Author:
Jan de Boer

Supervisor:
Dr. Ir. C. J. G. Onderwater
Second examiner:
Dr. Ir. J. P. M. Beijers

Abstract

In contemporary high-energy physics experiments, Particle IDentification (PID) is decisive in accurate reconstruction of rare interactions. Observed mass spectra are sensitive to errors arising from backgrounds, for instance due to a particle misidentification. It is of interest to simulate such processes in order to subtract it from the signal to improve its quality. The effect of misidentification upon such a background signature in the curious case of an anisotropic decay has raised attention lately. Limited to two-body decays, the main objective of this thesis is to explore an origin of anisotropy in the emission distribution of the center-of-mass frame and to simulate the corresponding effect upon an energy distribution due to particle misidentification.

July 7, 2017

It is wrong to think the task of physics is to find out how nature is. Physics concerns what we say about nature.

-Niels Bohr

Author: Jan de Boer

Student number: S2381842
Contact:: j.de.boer.42@student.rug.nl

Contents

1 Introduction

Nowadays, in the field of high-energy physics (HEP) dedicated experiments test the Standard Model (SM) at high accuracy through the study of rare interactions. As the name suggests, typical interactions of extraordinary nature do not generally appear. Experiments are operated at increasing energies, allowing such phenomena to occur more likely. In addition to this, the frequency of collisions can be as high as tens of megahertz in order to gain sufficient amount of data. This is needed if one wants to establish the high statistical significance demanded for these studies. Upgrades to both accelerators and detectors are crucial to sustain accurate and efficient operation. Optimization of strategies and methods to register and reconstruct events as fully as possible are achieved by combining multiple information sources. In addition to tracking and calorimetry, Particle IDentification (PID) is a crucial aspect of most particle physics experiments[1].

The invariant mass spectrum in the decay processes are of interest since it corresponds to the mass of the unstable particle. In particular, for the high precision experiments the exotic states created are of such short lifetime that one is not able to observe them directly. With information obtained from its decay products one is able to reconstruct the invariant mass spectrum, though this is sensitive to numerous errors. To achieve a clearer invariant mass signal, particle identification has been proven an effective method to correct for such errors. To study the signature of these backgrounds, one can mainly subdivide them in three categories: peaking backgrounds, semi-peaking backgrounds and combinatorial backgrounds. Shortly, the first appear due to particle misidentification(s) in a decay, the second when a decay is identified as a signal with one or more missing decay products and the third arise when products of separate decays coincidentally combine such that they form a signal decay.

In this thesis the focus will be on peaking backgrounds due to misidentification of particles. The scope of the research is limited to two-body decays, which meet the criteria for a possible extension to an anisotropic decay distribution in the center-of-mass (CM) system. In the first section material is presented for further understanding and the need of sophisticated identification methods. Next, the second section introduces a calculation of general decay rate, after which a section on the kinematics of a two-decay decay follows. Reconstruction of the invariant energy will be treated, together with the effect of a misidentification on the invariant energy. To conclude, the last section of the main core of this thesis is dedicated to asymmetrical behaviour and its effect upon energy distributions.

2 Event Reconstruction

In high-energy physics an event is the experimental result of an interaction during the collision of particles in an accelerator[2]. The product of an interaction can be up tens or even hundreds of secondary particles, resulting in a considerable volume of data. At the Large Hadron Collider (LHC) the raw data of about 600 million events per second has to be processed. Filtering is done both through hardware and software to select only events of interest. Processing includes reconstructions such as particle trajectories, identifying particles and determination of vertices. Each type of particle has its characteristic signature, using various detectors one is able to accurately distinguish among them. Nevertheless, for high momenta, dedicated detectors are essential to perform sufficiently. This chapter mainly focuses on the identification of particles in such a reconstruction. The techniques used to reconstruct the invariant mass of a resonance, will be treated in the chapter on two-body decay.

Before turning focus on the several techniques used in reconstruction, it is useful to have a complete overview of a detector in mind. Although the sections will mainly use examples taken from the LHCb experiment, the project is not limited to the conditions and physics studied by this group.

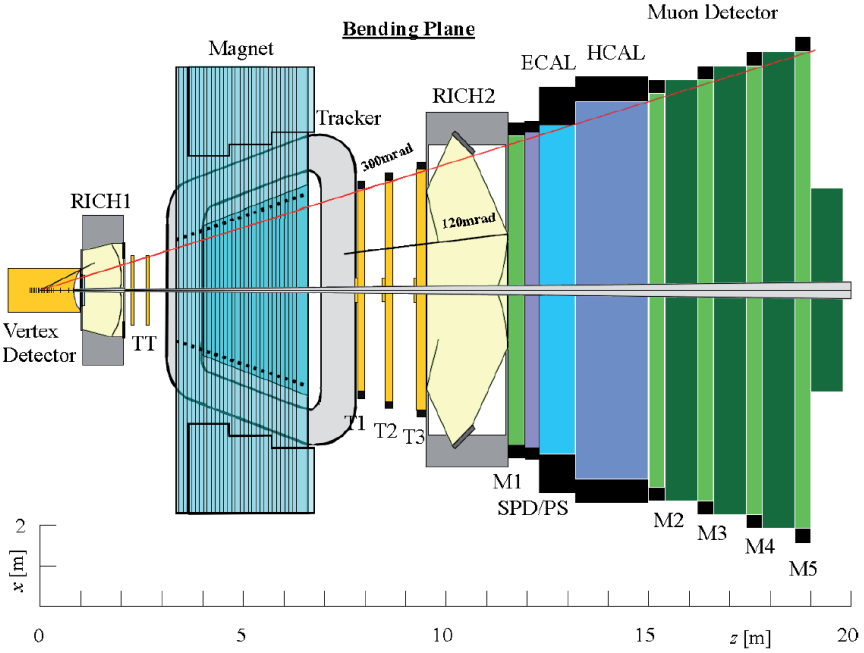

Figure 1: The LHCb detector: top view.

The separate parts of figure (1) will shed light on throughout the following paragraphs. Its design is a forward spectrometer, as the decay products of b hadrons are produced predominantly with high momentum and low polar angles.

2.1 Tracking System

The tracking system is used to reconstruction both vertices and trajectories of particles passing through the detector. Information on trajectories taken before and after going through the magnet allows for a particles momentum to be determined. The LHCb tracking system consists of the following components: Vertex Locator (VELO), Tracker Turicensis (TT), dipole magnet and tracking stations T1, T2 and T3. The VELO provides measurements of track coordinates which are use to identify the primary interaction vertices and the

secondary vertices that are a distinctive feature of b- and c-hadron decays[3]. Combining decay length and a particles -factor, one can accurately determine its lifetime. The track finding algorithms in LHCb start with a search in the VELO detector for straight lines. These tracks are then combined with hits in the tracking stations to produce the "long" tracks that are used for most physics analyses. The track fit is performed using a Kalman fit[3].

2.2 Particle Identi cation

Particle identification (PID) is the full procedure of accurately distinguishing between long-lived particles (; K; p; e; and). For a 'traditional' experiment the signature of each of the particles can be seen in the following figure:

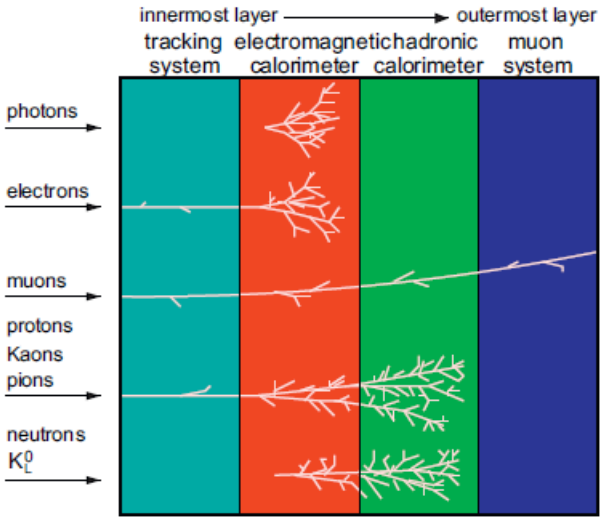

Figure 2: Signatures of particles in various detector layers, obtained from ref [1].

The particles of particular interest in this project are and K, since a hadronic decay will be considered later on. p together with and K, show very similar characteristics at high momenta and hence, it will be more difficult to separate one from another. At LHCb PID analysis is done by combining information from the following sub-detectors: Ring Imaging Cherenkov detectors (RICH1 and RICH2), muon chambers (M1 - M5) and calorimeter system (SPD/PS, ECAL, HCAL). The main focus will be on RICH and briefly treat the muon chambers and calorimeter system.

2.2.1 RICH

The Ring Imaging Cherenkov detectors are used to characterize and discriminate among charged hadrons at high energies. The RICH detectors comprises of two independent sub-detectors, namely RICH1 and RICH2, the first covers low momentum range 2 up to 40 GeV/c and the second a larger momenta range from 15 to 100 GeV/c. When a charged particle with velocity v traverses a dispersive medium of refractive index n, excited atoms in the vicinity fo the particle become polarized, and if v is greater than the speed of light in the medium c/n, a part of the excitation energy reappears as coherent radiation emitted at a chracteristic angle to the direction of motion[4]. The method based on the *cherenkov effect* is used to directly measure a particles speed

by determination of the angle $_c$ at which radiation is emitted. The obtained speed together with momentum measured by the tracking system can be combined to determine the mass. However, at high momentum the angle of emission narrows at high velocities and it becomes challenging to distinguish between the particles of interest.

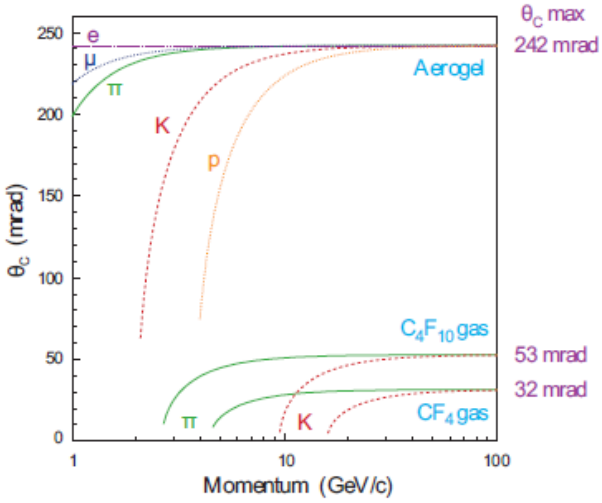

Figure 3: Cherenkov angle for the different particles as a function of momentum, obtained from ref [5].

The Aerogel, C_4F_{10}- and CF_4-gas in figure (3) are the mediums, corresponding to different index of refraction n, used in the RICH detectors to study the cherenkov radiation at a particular range of momenta. It is clearly visible that K separation show similar angle $_c$ towards 100 GeV/c momentum. Therefore, to distinguish a from a K or vice versa in this regime leads a higher rate of mis-identification as is shown in figure (4).

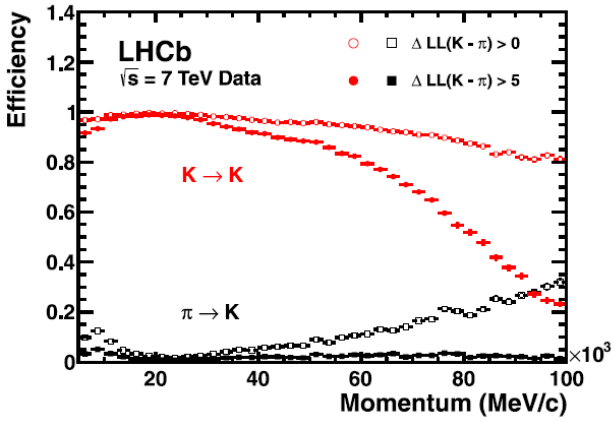

Figure 4: Kaon identification efficiency and pion misidentification rate measured on data as function of track momentum, obtained from RICH PID performance, ref [6].

The open and filled marker distributions are resulting from two different requirements imposed on the data. From the data, kaon identification efficiency averaged over the momentum range 2-100 GeV/c, was

found to be 95% with a 10% pion misidentification fraction. The misidentification rate is not only a function of momentum, also track multiplicity has an effect on the efficiency. Therefore at higher event rates, the rate of misidentification of a pion increases.

2.2.2 Calorimeter System

This system provides identification of photons, electrons and hadrons as well as their specific energy loss dE/dx and positions. The calorimeter system consists of following detectors: scintillator pad detector (SPD), pre-shower detector (PSD), electromagnetic calorimeter (ECAL) and hadron calorimeter (HCAL). Hadronic showers have different characteristics than electromagnetic showers, hence precise measurements are done by separate dedicated detectors. Again from dE/dx information a particles velocity can be determined and when combined with its momentum, the rest masses can be found. Particular for low momenta (up to 30 GeV/c) this can be used to identify particles.

2.2.3 Muon chambers

Identification of muons is of special interest in the experiments done at LHCb, as they are present in several decay products of b hadrons. As muons are long lived and highly penetrating, the muon system is furthest away from the interaction point. It provides momentum measurement by station M1, placed before the calorimeter, and stations M2 - M5. Combined, again track reconstruction is done and which requires a hit in all five stations.

This concludes the section on particle identification techniques, as mentioned we will make use of a misidentifaction to see what the effects in a reconstruction of a decay will be. Before going on to the kinematics, the next chapter will treat the main aspects that contribute in calculating a decay rate.

3 Decay Rate

In accelerators relativistic collisions between two particles are studied. These collisions can be divided into categories, in which *interactions* are studied. As we will see in this chapter, it is due the laws of conversation of energy and momentum that these classifications of collisions arise and one can distinguish among them. After being acquainted with the general part on processes, we will have a closer look into two particles processes.

3.1 Interaction and Decay Processes

Characteristics of interactions are generally studied by collisions between two elementary particles A and B. In classical collisions both mass and momentum need to be conserved and when shifting to relativistic collisions, mass is exchanged by energy. To be consistent energy is referred to as the total energy of a particle, i.e. rest energy (mass) plus kinetic energy. By the laws of conservation of energy and momentum, one can divide interactions into the following three categories: *elastic, quasi-elastic and inelastic*. Each will individually considered. Elastic scattering can be depicted as

$$A + B \;!\; A + B: \tag{1}$$

Both the number of particles and type do not change in the interaction. Therefore, in such a scattering process only the momenta of particles A and B change. In quasi-elastic scattering two final particles C and D are produced out of the interaction of particles A and B. In contrast to elastic scattering the initial types of particles differ from the final ones:

$$A + B \;!\; C + D: \tag{2}$$

Also, it might happen for example that one of the initial particles changes into to other one during the process. Finally, the most common type of scattering is inelastic:

$$A + B \;!\; C + D + E + F + :::; \tag{3}$$

in which the final state consists of multiple particles. At high energies this type is dominant if A and B are strongly interacting particles. The number of final state particles in an ordinary process can be tens and even hundreds[7].

Kinematically, the decay of an unstable particle A differs from the above as the initial state consists of only one particle.

$$A \;!\; B + C + D + ::: \quad : \tag{4}$$

Equations (1)-(4) are allowed for only those interactions that satisfy the laws of conservation of momentum and energy and several other conservation laws (i.e. electric charge, baryon and lepton numbers, parity, angular momentum etc.). For now we are only interested in the kinetics of a reaction, therefore the laws of energy and momentum conservation will be of importance as we will be come across them throughout later sections. As introduced earlier these symmetries due to the fact we live in 4 dimensional space-time, known as Minskowski space. The *four-momentum conservation* can be expressed in a single line:

$$\sum_{i=1} p_i = \sum_{f=1} p_f; \tag{5}$$

p is a four-vector and p_i and p_f are the 4-momenta of the initial state and final state particles. This can also be written as conservation laws of each the individual components, of which three momentum and one energy:

$$\begin{aligned} \sum_{i=1} E_i &= \sum_{f=1} E_f \\ \sum_{i=1} p_i &= \sum_{f=1} p_f \end{aligned} \tag{6}$$

together with

$$E_i^2 = \mathbf{p}_i^2 + m_i^2; \qquad i = A; B; C; :::; N \tag{7}$$

Are all the relations used to define a specific process. Bold p is used to emphasize a momentum vector, p is corresponding to a four-momentum vector. Summation is taken over the primary and secondary particles. One can describe the equations (1)-(4) kinematically, with the proper numbers of particles taken in both initial and final states. Together these conservation laws restrict and forbid many processes of particle interactions. The above relations will be used in the following sections, in which decay processes will be considered more profoundly.

3.2 Total Decay Rate

Evaluating scattering processes often involves calculating decay rates (Γ) or scattering cross sections ( ). To do so, the kinematics lack the necessary information to obtain a full description. We need to include the *amplitude* M, which contains all the dynamical information. We can calculate it by evaluating the relevant Feynman diagrams, using the *Feynman rules* appropriate to the interaction in question[8]. Together with the *phase space* available, the total decay rate can be explicitly calculated by inserting both quantities in Fermi's *Golden Rule*. This will be explicity done for a spinless decay at the end of this paragraph to illustrate the associated physics.

3.2.1 Decay and Lifetime

In accelerators one studies phenomenology under highly energetic conditions. Particles created in a collision are usually of exotic and unstable nature, that is to say their lifetimes are very short. Strictly, one means the *average* lifetime of a large sample of particles when referring to a particles lifetime. The probability of a particle disintegrating in the next microsecond is independent of its age. This leads to an equal probability for each particular particle to decay at each instant of time. This is expressed as the *decay rate* Γ, the *probability per unit time* that any given particle will decompose. For a sample $N(t)$, where N is the number of particles at time t, $N\Gamma dt$ is the number of decaying particles in a infinitesimal time dt. Evidently, this would lead to a decrease of the sample:

$$dN = \quad \Gamma N dt \qquad N(t) = N(0)e \quad ^{t} \tag{8}$$

The number of particles left decrease exponentially with time. From this a particles lifetime can be deduced, which is simply the reciprocal of the decay rate:

$$= \frac{1}{\Gamma} \tag{9}$$

Most particles have various *modes* to decay, a mode is a unique set of both the primary particle as well as the

secondaries. The decay rate of a single parent particle depends on the mode it decomposes into, and hence on the secondary particles involved in the disintegration of a primary. For this reason it is practical to define the *total* decay rate to be the sum of the individual decay rates;

$$\Gamma_{tot} = \sum_{i=1}^{\infty} \Gamma_i \tag{10}$$

and

$$= \frac{1}{\Gamma_{tot}} \tag{11}$$

As a particle has various decay modes, the fraction of all particles that decompose into a given set of secondaries is called *branching ratio*. Branching ratios are of particular interest to probe the standard model via rare modes. The branching ratio for a particular mode is determined by the following manner:

$$B = \frac{\Gamma_i}{\Gamma_{tot}} = \Gamma_i \tag{12}$$

Once one has obtained the decay rate Γ_i for each mode, it follows by using the listed equations above, one can determine properties such a lifetime and branching ratios. For scattering processes similar concepts apply, with the initial state consisting of two particles.

3.2.2 Phase Space

Imposing conservation of four-momentum leads to constraints on the final state particles. These four relations formed by equations (6)-(7) are of purely kinematic nature and relate the primary to secondary particles. It is of interest to determine how many independent kinematic variables are needed to fully describe the kinematic states of a decay. For the description of a 1 ! n decay, 3(n + 1) components of their momenta are needed. A way of dealing with such a process is to choose a convenient reference frame. The rest frame of unstable particle A is defined such that

$$E_A = m_A; \quad p_A^* = 0;$$

which translates into imposing the sum of the momentum of secondaries to be 0. 3n kinematic variables describe the final states and together with the conservation laws, 3n - 4 of them are independent. For a two particle decay (n = 2), only two essential variables remain. These kinematic variables turn out to be the invariant particle masses of the secondaries.

The unconstrained 3n dimensional space of the final state momentum $\boldsymbol{p}_f$ is called momentum space. The union of momentum and configuration (coordinate) space of all particles in a physical system is termed the phase space[9]. This is the 3n - 4 dimensional surface within momentum space. From the statistical ensemble we know that the number of quantum states of a free particle in the volume element of its phase space is

$$dN = \frac{d^3p dV}{2\ ^3} \tag{13}$$

The probability of quantum particle production is proportional to the number of quantum states in which this particle may occur. The probability of occurrence of a certain number of particles in the interaction process is in turn proportional to the product of their phase volumes divided by $(2\ )^{3n}$, where n is the number of secondary particles. At experiments secondary particles can be considered as free particles, and their coordinate wave functions are plane wave that correspond to the states of particles with certain momenta[10]. The particles are confined in a volume V and the corresponding states are wave functions normalized to this volume. The

associated production probability of a particle is obtained by computing the squared modulus of the wave functions, which results in a factor V^{-1}. Returning to equation (13), the volume of the *configuration* space $V = \int dV$ is always canceled by the factor V^{-1} resulting from the normalization. Therefore the probability is described only by the volume elements of *momentum* space of the secondary particles. Again, applying the conservation laws of energy and momentum, a four-dimensional δ-function needs to be added to the resulting product of volume elements of momentum space. The result is a named the phase-volume element of the secondary particles:

$$d\Phi = \prod_f \frac{d^3p_f}{(2\pi)^3} (2\pi)^4 \delta^{(4)}\left(\sum_i p_i - \sum_f p_f\right) : \tag{14}$$

, The factor $(2\pi)^4$ is front of the δ-function is introduced arbitrarily. Phase-volume is a non-invariant quantity. In the relativistic regime, the wave functions not only contribute volume factors when normalized, but also energy dependent factors $(2E)^{-\frac{1}{2}}$). By computing the squared modulus of this wave we can now obtain an expression for the relativistically *invariant* phase volume of the secondary particles

$$d\Phi = \prod_f \frac{d^3p_f}{2E_f(2\pi)^3} (2\pi)^4 \delta^{(4)}\left(\sum_i p_i - \sum_f p_f\right) \tag{15}$$

This is the general result, which will used in order to state the golden rule for a specific process. The remainder of this paragraph will be dedicated to explicitly stating the invariance of equation (15) guided by the book of Gol'danskii[7].

The invariance of equation (15) will be shown by dividing $d\Phi$ into invariant fragments. The four-dimensional δ-function is invariant.

$$\delta^{(4)}\left(\sum_i p_i - \sum_f p_f\right) = \delta\left(\sum_i E_i - \sum_f E_f\right) \delta^{(3)}\left(\sum_i p_i - \sum_f p_f\right)$$

The momentum-space volume can also be written in an invariant form:

$$\int \frac{d^3p_f}{2E_f} = \int d^4p_f \ \delta(p_f^2 - m_f^2) \tag{16}$$

In this derivation there is made use of (7), together with the following relation

$$\int [f(x)]dx = 1/|f'(x)|_{x=x_0}; \tag{17}$$

where f'(x) is the derivative is taken at the point $x = x_0$, where $f(x_0) = 0$.

3.2.3 Amplitude

It is mentioned before that the *amplitude* M contains all the *dynamics* of scattering and decay processes. Naturally it is a function of the momenta of both initial and final state particles. It gets more complicated when one has to include the spin of the particle, the basic scalar field theory only applies in case of a spinless scalar particles. Interactions between particles of different nature and the number of particles drastically increases the calculations to be done for explicit computation. Calculations can be shortened by evaluating the appropriate Feynman diagrams. These diagrams are well known today and come with the so called 'Feynman rules'; using them saves enormous effort. For a given theory, let's say a ^{3} which can be interpreted as a spinless two-body decay, one has to do all the calculations. From the result one can assign the various parts of the obtained mathematical expression to a schematic part of the process, known as 'Feynman diagrams'. The one shown below is for the lowest order contribution of a ^{3}-theory

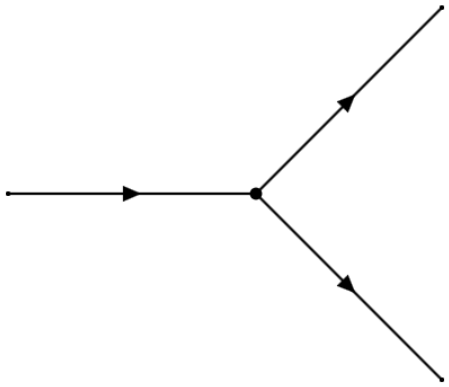

Figure 5: Feynman diagram for a ^{3}-theory

Higher order terms typically correspond to more complicated diagrams in which for example self interaction occurs. As one should expect, higher order terms are the more exotic processes which should result in a small amplitude for it is unlikely to occur. It is this origin that translates itself to the branching ratios, as discussed in the paragraph on decay rate. The role of the amplitude is not unexpected since we already stated this at the very beginning of this section. Without further introducing the corresponding rules of a scalar ^{3}-theory, it turns out that only one rule applies for such decay[8], resulting in:

$$M = ig \tag{18}$$

This concludes what is relevant in order to turn to the calculation of a decay rate Γ.

3.2.4 Golden Rule for Decay

This paragraph concludes the section by computation of a scalar two-body decay. Although not used later on, it illustrates some important aspects which are of interest for particles carrying spin. The decay rate for an unstable particle has been earlier defined as the probability per unit time that a particle will disintegrate. Consider the decay of a particle A to an unknown number of secondaries

$$A \;!\; B + C + D + \ldots \tag{19}$$

along with the corresponding formula:

$$d\Gamma = d! = \frac{s_A s_f |M|^2}{2E_A(2S_A+1)} \prod_f \frac{d^3p_f}{2E_f(2\pi)^3} (2\pi)^4 \delta^{(4)}\left(p_A - \sum_f p_f\right) \tag{20}$$

for an arbitrary coordinate system. This is the differential probability per unit time for a given particle A to decay into a number of secondaries. To obtain the total decay probability one has to integrate over the momenta of the secondary particles. The probability is taken account for by the phase volume on the right hand side, is restricted by the conservation laws through the delta function. The summation in front of the modulus of the squared amplitude is taken over the spin states of the secondary particles (S_f) and unstable particle A (S_A). Thus far, all these quantities are invariant quantities, except for the factor of $2E_A$ in the denominator. The energy E_A depends on the frames of reference in which the decay is studied. This elegantly shows the dilation effect on a particles lifetime. Let's examine equation (20) for a two particle decay. To be consistent with previous sections, subscript A of the unstable particle will be dropped and the secondary

particles B and C will be denoted with subscript 1 and 2 respectively.

$$d\Gamma = d! = \frac{s s_1 s_2 |M|^2}{2E(2S+1)} \quad \frac{d^3p_1}{(2\ )^3 2E_1} \frac{d^3p_2}{(2\ )^3 2E_2} \quad (2\ )^4\ {}^{(4)}(P \quad p_1 \quad p_2) \tag{21}$$

Where the sum over the spin states are neglected for the time being. When considering a two body decay the squared amplitude M is constant. As in (18) spinless particle will be taken into account only, resulting in:

$$d\Gamma = d! = \frac{|M|^2}{2E} \frac{d^3p_1}{(2\ )^3 2E_1} \frac{d^3p_2}{(2\ )^3 2E_2} (2\ )^4\ {}^{(4)}(P \quad p_1 \quad p_2) \tag{22}$$

As the leading variables in this integral are those from the *two-particle phase volume*, we are left with an expression which can be carried out exactly. Again this process will be evaluated in the rest frame (CM) of the unstable particle, as it is a convenient way of evaluating the phase volume $d\Phi$. Stating $d\Phi$ in this frame:

$$d\Phi = \frac{d^3p_1}{(2\ )^3 2E_1} \frac{d^3p_2}{(2\ )^3 2E_2} (2\ )^4\ {}^{(4)}(P \quad p_1 \quad p_2) \tag{23}$$

Both P and p are the 4-momentum, in the CM frame P^2 equal M^2, where M is the mass of the unstable particle. Furthermore, $p_1^* + p_2^* = 0$, $E_1 + E_2 = s^{\frac{1}{2}}$ and $E_i = (m_i^2 + (p_i^*)^2)^{\frac{1}{2}}$. The first statement can be used to evaluate the d^3p_2 integral by considering ${}^{(4)}$-function. Applying only the part of momenta one can eliminate the integration of d^3p_2, we obtain

$$d\Phi = \frac{d^3p_1}{(2\ )^6 2E_1 2E_2} (2\ )^4\ (M \quad E_1 \quad E_2) \tag{24}$$

As a consequence E_2 is now rewritten as $[E_1{}^2 + m_2^2 \quad m_1^2]^{\frac{1}{2}}$. We continue by changing the integration to spherical coordinates; $d^3p_1 = |p_1^*|^2 d|p_1| d\cos\ {}_1 d\ {}_1$. $p_1 dp_1 = E_1 dE_1$ using $E_1^2 = p_1^2 + m_1^2$ and hence, $|p_1^*| E_1 dE_1 d\Omega_1$, where $d\Omega_1 = d\cos\ {}_1 d\ {}_1$ is the solid angle of emission of particle 1. Substituting this in equation (24) results in:

$$d\Phi = \frac{|p_1^*| dE_1 d\Omega_1}{(2\ )^6 4E_2} (2\ )^4\ (s^{\frac{1}{2}} \quad E_1 \quad E_2) \tag{25}$$

To perform the last part we evaluate dE_1 by using the identity (17) again, where the root of the $(s^{\frac{1}{2}} \quad E_1 \quad E_2)$ is obtained by substituting E_2 in terms of E_1 and both masses of the 2 particles. The root of this function is[7]:

$$\begin{aligned} E_1 &= \frac{s + m_1^2 \quad m_2^2}{2s^{\frac{1}{2}}} \\ &\textit{and} \\ E_2 &= \frac{s + m_2^2 \quad m_1^2}{2s^{\frac{1}{2}}} \\ |p_1^*| &= \frac{[s \quad (m_1+m_2)^2]^{\frac{1}{2}} [s \quad (m_1+m_2)^2]^{\frac{1}{2}}}{2s^{\frac{1}{2}}} = \frac{^{\frac{1}{2}}(s; m_1; m_2)}{2s^{\frac{1}{2}}} \end{aligned} \tag{26}$$

$$d\Phi = \frac{|p_1^*| d\Omega_1}{(E_1+E_2)(2\ )^6 4E_2} (2\ )^4 \tag{27}$$

$$d\Phi = \frac{^{\frac{1}{2}}(s; m_1; m_2)}{2s} \frac{(2\ )^4}{(2\ )^6} d\Omega_1 \tag{28}$$

The * remind us that we considered phase volume in the CM frame. From the conservation laws on energy and momentum no further restrictions are imposed on the emission angles $_1$ and $_1$. As the amplitude M is a constant, for a two body decay of scalar particles one can integrate over $d\Omega_1$ as:

$$\begin{aligned} d\Phi &= \frac{^{\frac{1}{2}}(s; m_1; m_2)}{2s} \frac{(2\ )^4}{(2\ )^6} 4 \\ d\Phi &= \frac{^{\frac{1}{2}}(s; m_1; m_2)}{2s} \end{aligned} \tag{29}$$

Inserting this result simultaneously with M = g back into equation (22) results in the final statement:

$$\Gamma = \frac{g^2\ \ ^{\frac{1}{2}}(s; m_1; m_2)}{8\ \ M^2}; \tag{30}$$

and for our interest there is no angular dependence in the differential decay rate.

$$\boxed{\frac{d\Gamma}{d\Omega} = \frac{g^2\ \ ^{\frac{1}{2}}(s; m_1; m_2)}{32\ \ ^2 M^2}}$$

This concludes the section on the decay rate, where we have been introduced to the main aspects to be taken into to account for the calculation of a particular decay mode. It is now time to examine a decay in various reference frames along with the consequences due to different observations, moreover it is of interest how one can relate these observations using transformations. Also, we will study the effect of a particle misidentication on the reconstruction of the invariant mass.

4 Boosting Two-Body Decays

The previous chapter has served to illustrate the amount of physics taken into account at the various steps of calculating a decay rate. Explicitly treating a particle decomposing into two secondaries, it proved that such a process is fully determined by the kinematics. Hence, it is useful to consider the kinematics thoroughly for the study of *two-body decays*. Once established, it will we followed by exploring the effects of applying a Lorentz boost to a particles rest frame and the proper way of relating the process in different reference frames. In this section we will study and use the following decay:

$$\begin{array}{ccccc} - & ! & {}^{0} & + & - \\ 1{:}3217 & ! & 1{:}1157 + 0{:}1396 & & (\mathit{rest}\quad \mathit{mass}\quad \mathrm{GeV}/c^2) \\ 1/2 & ! & 1/2 & +0 & (\mathit{intrinsic}\quad \mathit{spin}) \end{array}$$

4.1 Energy and Momentum in CM frame

Once again, consider an unstable particle A decay into two secondary particles 1 and 2:

$$A \;!\; 1+2{:}$$

In the rest frame of particle A this can be studied rather quickly. The corresponding 4-momentum of particle A $(E;P)$ is defined to be $(M;0)$ in this frame. The 3-momentum of particle A is $p_A^* = 0$ by the laws of conservation of momentum the following relations hold for the 3-momenta of the secondaries:

$$p_1^* + p_2^* = 0{:} \tag{31}$$

Thus, the momenta are of equal magnitude but of opposite directions;

$$\begin{aligned} |p_1^*| &= |p_2^*| \\ p_1^* &= \quad p_2^* \end{aligned} \tag{32}$$

Using the momenta, the corresponding energies of the particles can be related using the known equation;

$$E_i = [p_i^2 + m_i^2;]^{\frac{1}{2}} \qquad i = 1;2{:} \tag{33}$$

The energies E_1 and E_2, and therefore the corresponding momentum $|p_1^*|$, are related to particle A by the law of conservation of Energy:

$$p_{\overline{s}} = M = E_1 + E_2 \tag{34}$$

In the rest frame of the unstable particle the CM energy $p_{\overline{s}}$ is equivalent to M. The $p_{\overline{s}}$ is the magnitude of the total energy in the CM system and therefore, it determines whether certain reactions are allowed. The equations are all there is for the given process. Although there is not much of complexity involved, it is worthy to spend a few words on the them. Once the particles are identified, their corresponding masses can be inserted into the formula's. By doing so, the keen eye immediately notices that the process is fully determined by now. As equation (33) for both particles 1 and 2 are left to one and the same momentum p_1^*, which in turn is determined by equation (34), due to the conservation law of energy. Derived from a different perspective, it is noteworthy that an equivalent statement was already made in the section on phase space. Since both energy and momentum of the secondary particles are determined by both their masses, as a consequence one would like to express them in terms of mass only. A convenient method to conduct such a derivation, is using the invariance of four momentum:

$$P = p_1 + p_2 \tag{35}$$

where $P; p_1; p_2$ are the 4-momenta of the particles. Rearranging this expression, followed by squaring both sides leads to:

$$\begin{aligned} p_2 &= P \quad p_1 \\ p_2^2 &= (P \quad p_1)^2 \\ p_2^2 &= P^2 + p_1^2 \quad 2M E_1 \\ m_2^2 &= M^2 + m_1^2 \quad 2M E_1 \\ E_1 &= \frac{M^2 + m_1^2 \quad m_2^2}{2M}: \end{aligned} \tag{36}$$

Similar, for particle 2 this yields:

$$E_2 = \frac{M^2 + m_2^2 \quad m_1^2}{2M}: \tag{37}$$

These equations directly relate the particles energy in the center of momentum frame to the particle masses, as demanded. The associated momentum can be obtained using the energy expression just derived together by nothing that m_1^2 can be written as $\frac{4M^2 m_1^2}{4M^2}$ and insert them into equation (34):

$$\begin{aligned} \mathbf{p_1^2} &= \frac{4M^2 m_1^2}{4M^2} \qquad \frac{M^2 + m_1^2 \quad m_2^2}{2M} \quad ^2 \\ \mathbf{p_1^*} &= \frac{\frac{1}{2}(M; m_1; m_2)}{2M} \end{aligned} \tag{38}$$

with $(M; m_1; m_2)$ corresponding to the kinematic function $(x; y; z) = x^2 + y^2 + z^2 \quad 2xy \quad 2yz \quad 2zx$. A consequence is that $M \quad m_1 + m_2$, which can be more easily seen after rewriting the above formula as:

$$\mathbf{p_1^*} = \frac{([M^2 \quad (m_1 \quad m_2)^2][M^2 \quad (m_1 + m_2)^2])^{\frac{1}{2}}}{2M}; \tag{39}$$

hence, for a particle particle to decay it must exceed the masses of the secondary particles. Finally, to conclude the section, the following reaction is introduced:

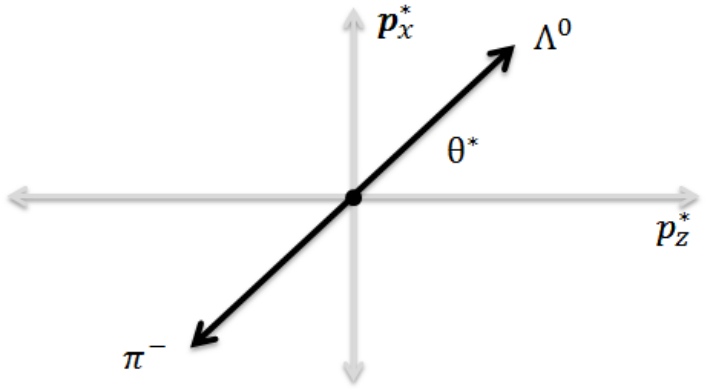

Figure 6: Decay of Xi to Lambda and Pion in CM frame.

$$\Xi \quad ! \ \Lambda^0 + \tag{40}$$

This decay is of particular interest since it meets the future criteria for a non-isotropic distribution. Hence, it will serve as a reasonable example for the further study of the characteristics of a two-body decay. First, it is time to have a look at what energies correspond to the decay under attention. For this we insert the masses of all particles involved in the process into the derived equations (36), (37) and (38). The masses are m = 1.3217 GeV, m = 1.1157 GeV and m = 0.1396 GeV. We obtain

$$E = \frac{M^2 + m^2 \quad m^2}{2M} = 1{:}124 \quad \text{GeV}$$

$$E = \frac{M^2 + m^2 \quad m^2}{2M} = 0{:}197 \quad \text{GeV}$$

$$p^* = p^* = \frac{\frac{1}{2}(M \;; m \;; m \;)}{2M} = 0{:}139 \quad \text{GeV}/c$$

This concludes the kinematics in the CM frame, next we consider the process as it is observed by the detector.

4.2 Energy and Momentum in Lab frame

In a detector the unstable particle A is moving at high velocity and as a consequence, secondary particles gain momentum as a due to the conservation laws. The energies measured are frame dependent and the commonly used name for the frame assigned to the detector is the Lab frame. A detector could for example measure a particles momentum by recording its momentum before and after it went through a magnet. The determination of it's mass can be done using the discussed methods in the PID section. In this section the kinematics of reaction (40) will be used to study the effect under a Lorentz boost upon the angles of emission of the secondaries. For this we picked an arbitrary angle of emission for the Lambda to be $_0 = 40$, and consequently for the Pion = 140 with respect to the z-axis. To apply the Lorentz boost (see (A.2)) with respect the the z-axis, we explicitly write the components of the for momentum as follows:

$$\begin{array}{ll} p_x = p \sin = 0{:}090 \quad \text{GeV}/c & p_x = p_x = 0{:}090 \quad \text{GeV}/c \\ p_z = p \cos = 0{:}107 \quad \text{GeV}/c & p_z = p_z = 0{:}107 \quad \text{GeV}/c \\ E = 1{:}124 \quad \text{GeV} & E = 0{:}197 \quad \text{GeV} \end{array}$$

The minus signs refer to the orientation with respect to the x- and z-axis. Next, we choose to boost the CM frame along the z-axis and with a -factor of 20. The energy and momentum of the unstable particle are determined this way. Normally, one refers to a particle of a certain energy which corresponds to a specific boost, which is the way it is observed in a detector. From there one needs to determine how to boost it to its own rest frame, in contrast to the procedure taken here. For the Ξ the quantities look as follows:

$$\begin{aligned} &= 20 \\ E = M &= 26;434 \quad \text{GeV} \\ &= \frac{p}{E} = 0{:}9987 \end{aligned}$$

We can use these and calculate the momenta in the lab frame using the proper Lorentz transformations, evidently the x-components remain unchanged. With this, one can calculate the corresponding angle of emission as measured by the detector:

$$\begin{aligned} p_x = p_x &= 0{:}090 \quad \text{GeV}/c \\ p_z = (p_z + E \;) &= 24{:}596 \quad \text{GeV}/c \\ = \arctan \frac{p_x}{p_z} &= 0{:}21 \end{aligned} \tag{41}$$

Likewise this can be done for the pion:

$$\begin{aligned} p_x &= p_x = 0.090 \quad \text{GeV}/c \\ p_z &= (p_z + E) = 1.805 \quad \text{GeV}/c \\ &= \arctan \frac{p_x}{p_z} = 2.85 \end{aligned} \tag{42}$$

Thus the pion is now boosted in the forward direction, with an angle of emission of -2.85 degrees relative to the direction of motion of Ξ. The lambda is emitted at an angle of 0.21 degrees. These values can be combined to form a quantity known as *opening angle*, which in the case of a -factor of 20 and = 40 is 3.06 . In the lab frame this can be depicted as is shown by figure (7). The momentum z component of the lambda should be 13 times the length of the z component of the momentum of the pion. Hence, it is schematic of process and should not be interpreted as a physical real representation.

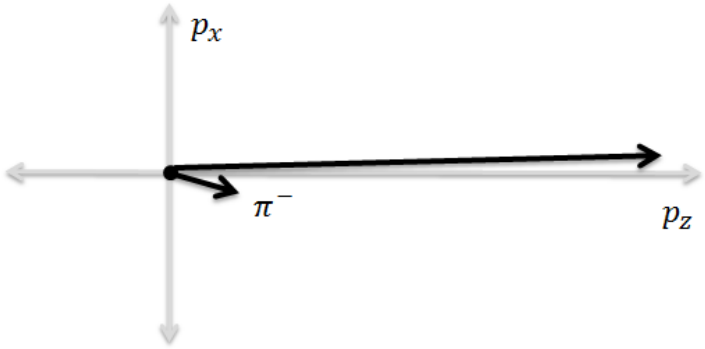

Figure 7: Decay of Xi to Lambda and Pion in Lab frame, schematically.

From the above transformations we may conclude that the opening angle is both dependant on and the energy of Ξ in the lab frame, and therefore the gamma factor. The demonstrate the influence of both quantities on the emission angles of and , the following graph is used:

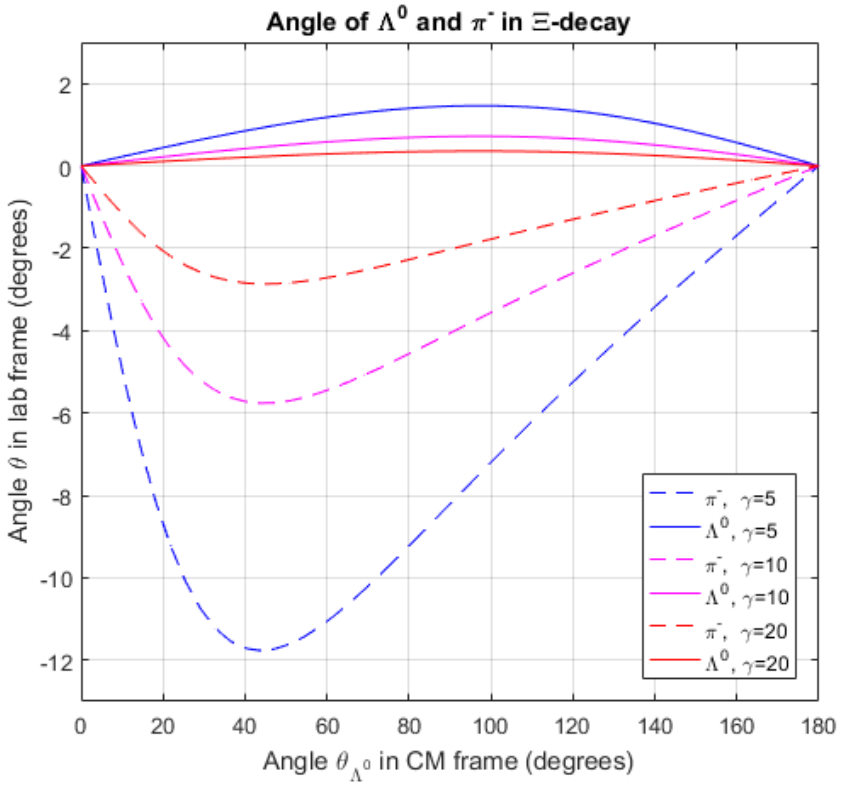

Figure 8: Emission angles as a function of and

Where one can read the computed angles from the red line at an angle of 40 degrees. It clearly shows the effect of boosting upon the opening angle, as it is squeezed narrowly at high energies. Another way of showing the effect of a Lorentz boost upon a center of mass distribution is shown in the following figure.

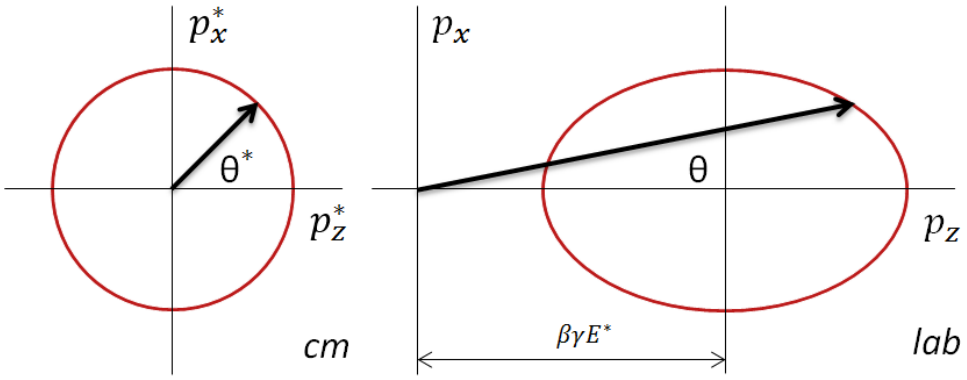

Figure 9: Lorentz transformation of isotropic -distribution

The non specified boost depicted in figure (9), shows a single particle and in contrast to figure (7) it covers 360 degrees. However, we can rotate around the figure z-axis without changing the energy, hence 180 degrees depicts the full spectrum. The effect of a Lorentz transformation upon such a distribution to the Lab frame

shows that angle now corresponds to two different momenta and hence, energies. The next paragraph will show how to apply the conservation laws to reverse the above process, in order the calculate mass of the unstable particle from the obtained data from the detector.

4.3 Invariant Mass Reconstruction

Relating the initial and final state of an interaction together with a specified mass of the unstable particle allowed us to fully determine the final state once the masses of the secondary particles were determined. In a detector one usually does not have all information on the initial state, and the final state is only known up to some accuracy. Measurements can only be done with a certain resolution, leading to uncertainties in the mass reconstruction of the unstable particle. In this paragraph we show the analytic approach to reconstruct the invariant mass. We start by stating the conservation of four momentum

$$P = p_1 + p_2; \tag{43}$$

and compute the invariant mass M as follows,

$$\begin{aligned} P^2 &= (p_1 + p_2)^2 \\ S &= m_1^2 + m_2^2 + 2(E_1 E_2 \quad jp_1 jjp_2 j \cos \ ) \\ E_i &= \quad \sqrt{p_i^2 + m_i^2}: \end{aligned} \tag{44}$$

Once m_i, p_i and *opening angle* have been determined, the invariant mass can be easily computed. The mass M appears as a delta peak in the energy spectrum. When including uncertainties this peak will be broadened, resulting in a width Γ in the invariant mass spectrum. The computation for the decay in case of a of 20 will perfectly deliver us the mass of the cascade. Also from the above equation, one is able to determine the gamma factor to transform and reconstruct the decay in the CM frame. For the analytic approach this can be used to check if we have acted correctly, since particles ought to be emitted back to back in this frame. In fact, one can just reverse the steps of the previous paragraph. Still using $= 40$ and a -factor of 20, we can use the above equations to computed the invariant mass. For this we use the obtained energies and momenta resulting from the boost to the Lab frame:

$$p^2 = p^2{}_x + p^2{}_z = 24{:}596 \quad \text{GeV/c}$$

$$p^2 = p^2{}_x + p^2{}_z = 1{:}807 \quad \text{GeV/c}$$

$$E = 24{:}6215 \quad \text{GeV}$$

$$E = 1{:}183 \quad \text{GeV}$$

Inserting them in the invariant mass formula, leads to:

$$\sqrt{S} = (m^2 + m^2 + 2(E \ E \quad jp \ jjp \ j \cos \ ))^{\frac{1}{2}} = 1{:}3217 \text{GeV/c}^2 \tag{45}$$

Which is exactly equal to the mass of the cascade. In the previous section it was derived that the opening angle in the Lab frame varies with the emission angle of Λ in the CM frame. Lets have a look what happens to our invariant mass as function of the emission angle.

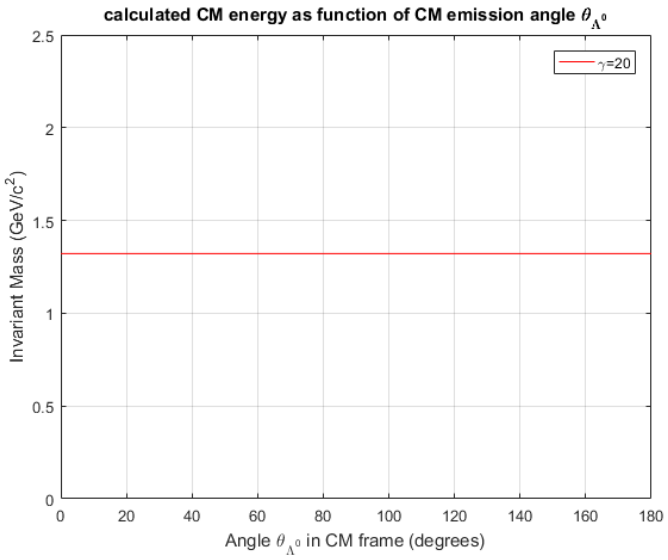

Figure 10: $p\overline{s}$ as a function of angle

It shows that there indeed is invariance of the mass, clearly independent of emission angle of Λ in the CM frame. For all emission angles we perform the reverse boost properly, when the particles have been identified correctly. This corresponds to the momentum circle from figure (9) being transformed to the correct origin. Next we consider the effect of a misidentification on the invariant mass spectrum.

4.4 Invariant Mass Reconstruction with mis-ID

For the reconstruction of a decay in which we have misidentified a for a K in the detector, we adjust the equations of the previous paragraph to include the extra mass, so that $m = m_K$ m . Including Λ and , this results in the expression

$$\begin{aligned} S &= m^2 + (m + m)^2 + 2(E E jp jjp j\cos) \\ E &= \sqrt{p^2 + m^2} \\ E &= \sqrt{p^2 + (m + m)^2}: \end{aligned} \tag{46}$$

We assume the determination of the particles momenta to be determined correctly. Using $m + m = m_K$, the equation can be written as

$$\begin{aligned} S^0 &= m^2 + m_K^2 + 2(E E_K jp jjp j\cos) \\ E_K &= \sqrt{p^2 + m_K^2} \quad with \quad p_K = p \end{aligned} \tag{47}$$

Clearly m is a positive value when misidentifying for a K, therefore S' will be overrated. The value of m $= 0.354$ GeV/c^2, we insert the known values from paragraph describing the decay in the Lab frame. This was for Λ emitted at an angle of $= 40$ and a -factor of 20. The corresponding opening angle was 3.05 , the calculated energies and momenta from applying a Lorentz boost to the CM frame are assumed to be obtained from a 'measurement'. This results in a center of mass energy of

$$S^0 = 4{:}967 \quad (\text{GeV}/c^2)^2; \tag{48}$$

and the corresponding resulting mass of the parent particle is determined to be

$$p\overline{S^0} = 2{:}229 \quad \text{GeV}/c^2{:} \tag{49}$$

Clearly, this differs from the value of 1.321 GeV, the actual rest mass of the cascade. As for the correct reconstruction, it is of interest to check whether there is an influence of the emission angle on the resultant invariant mass spectrum. This will be of importance when we deal with an anisotropic distribution, since the nature of the suppression depends what energy is filtered out of the invariant mass spectrum spectrum. The following figure shows the corresponding behaviour.

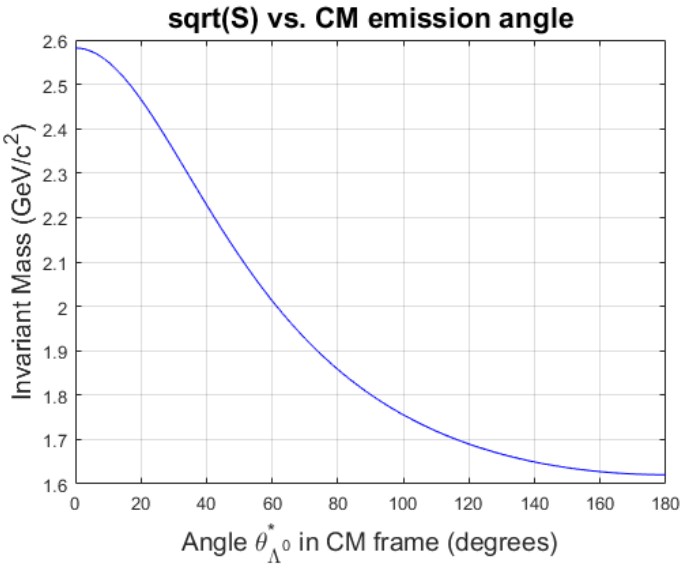

Figure 11: Invariant mass the cascade as a function of angle

The resultant 'invariant' mass spectrum changes roughly 1 GeV/c^2 as the emission of the lambda changes from forward direction to backward direction with respect to the z axis. The forward direction corresponds to the highest energy of 2.582 GeV/c^2, and the backward direction to an energy of 1.621 GeV/c^2. Moreover, the graph shows flattening near the maximum and minimum . Here the invariant mass stays close to these values for some range of emission angle. The next step is to translate this graph into a 'measurement', the intensity that a detector measures within a certain energy resolution, in the lab frame. For this we create particles isotropically emitted in de CM frame, to create 100 000 particles equally spread over 180 , there is 1 emission per -width of 0.0018 . Next, we determine the resolution of the detector to correspond to a resolution in the reconstructed energy to be 0.01 GeV/c^2. With such a resolution the detector counts the amount of particles within that energy range. The result of scanning over 180 is depicted as a histogram, representing the distribution from the above figure in the following way:

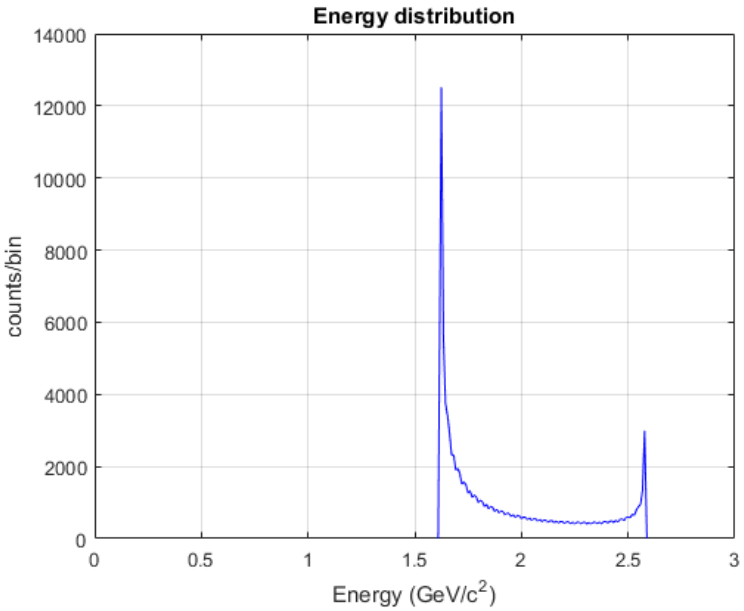

Figure 12: Intensity per energy range E = 0.01 GeV/c^2, N = 100000

Indeed, the resultant histogram perfectly depicts the predicted behaviour. When a detector is able to measure within a certain energy window together with its resolution, a reconstruction on the energy would lead to this distribution. For the studied decay, this would mean a window of about 1 - 25 GeV, the minimum and maximum energy of the secondary particles. Next, it is of interest to examine the effect of an anisotropy in the emission spectrum on the resultant distribution. Before going on, we want to conclude the section by stating what is done so far.

In this section we have boosted a two body decay with a -factor of 20 and from there we started the reconstruction of our CM energy, with the aim of finding the mass of the unstable particle. The opening angle in the lab frame was determined to be dependent on both the emission angle in the CM frame and the -factor we applied on the cascade. The $p\overline{S}$-formula resulted in two cases, one in which we identified the particles correctly and one in which a pion was identified as a kaon. Misidentification of a kaon translated itself in a m of +0.3541 GeV/c^2, the momenta were assumed to be determined correctly in *both* cases. The former lead to an invariant spectrum, independent of the emission angle in contrast to the latter, which showed dependence resulting in a spectrum with a width of roughly 1 GeV/c^2. To interpret this, a sample of 100 000 emissions was created to study this spectrum with a given energy resolution. The resultant histogram showed us two 'ears', one at maximum and the other one at minimum CM energy. The results of both reconstructions are depicted in the histrogram of figure (13).

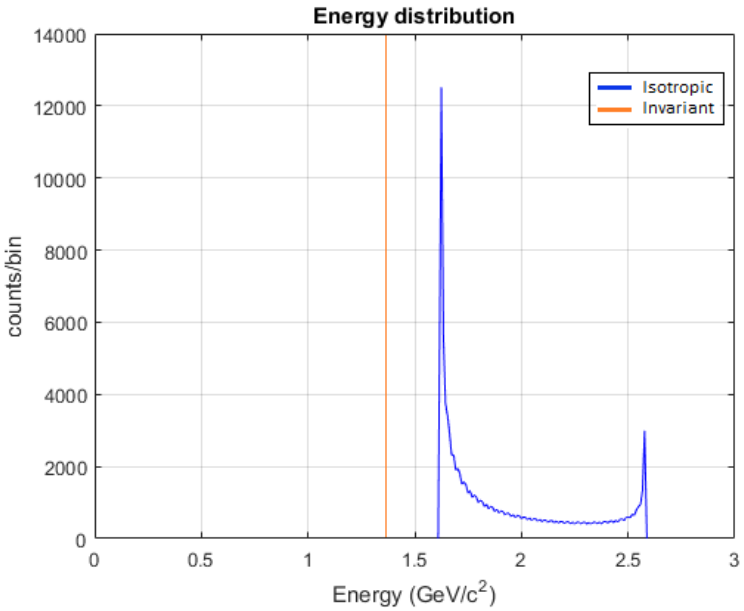

Figure 13: Invariant energy and isotropic distribution

It physically means that introducing extra mass leads to a wrong inverse boost. For correct identification and thus mass, the combination of energy and CM of mass energy lead to a correct inverse boost of 20 over all emission angles , ending up in the CM frame with an energy of 1.3217 GeV. This can be described as follows:

$$^{1} = \frac{E \quad + E}{p \quad \overline{S}} = 20 \tag{50}$$

Emphasizing that $p_{\overline{S}}$ has a dependence on the energies of the secondaries, which in turn depend on the emission angle , it is the *combination* of numerator and denominator that leads to a constant and correct inverse gamma factor. Introducing a m of +0.3541 GeV/c^2 changes this balancing act of the two secondaries, resulting in varying behaviour.

$$^{1'} = \frac{E \quad + E_K}{p \quad \overline{S'}} \; 6 = constant \tag{51}$$

The prime reminds us that the system we apply the inverse boost to has also been changed in overall energy due to the additional mass. The complex behavior results from the fact that the extra mass propagates in both numerator and denominator. The energy of the kaon depends on the emission angle and as we have seen $p_{\overline{S'}}$ varied 1 GeV/c^2 over 180 degrees. An analytic expression is lengthy and therefore excluded. The numerical computation is shown in the following figure.

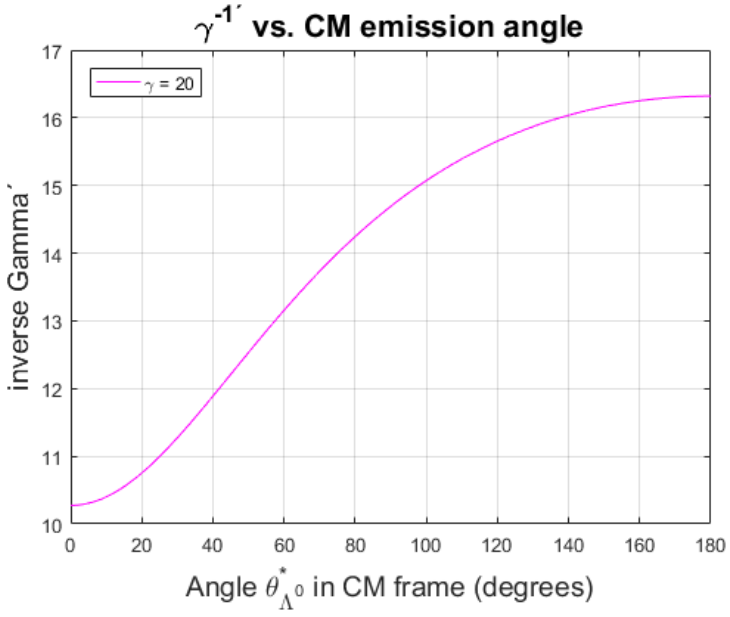

Figure 14: Inverse gamma as a function of angle

The inverse Lorentz transformation corresponds to an inverse gamma factor varying from 10.3 to 16.3 over the range of 180 degrees in emission angle . Thus, the effect of m upon the inverse gamma is strongest when the lambda is emitted in the direction of the velocity of the cascade, and therefore the additional mass in opposite direction, when reconstructed in the CM frame. The range is not high enough to end up in the CM frame, since it is too low the resultant invariant energy is estimated to high. The distribution of the inverse gamma factor is an indication that there is a spread in the invariant energy, which we have already seen from figures (11) and (12). In fact, there is strong correlation between the inverse gamma factor and the obtained invariant mass, as shown in the following figure:

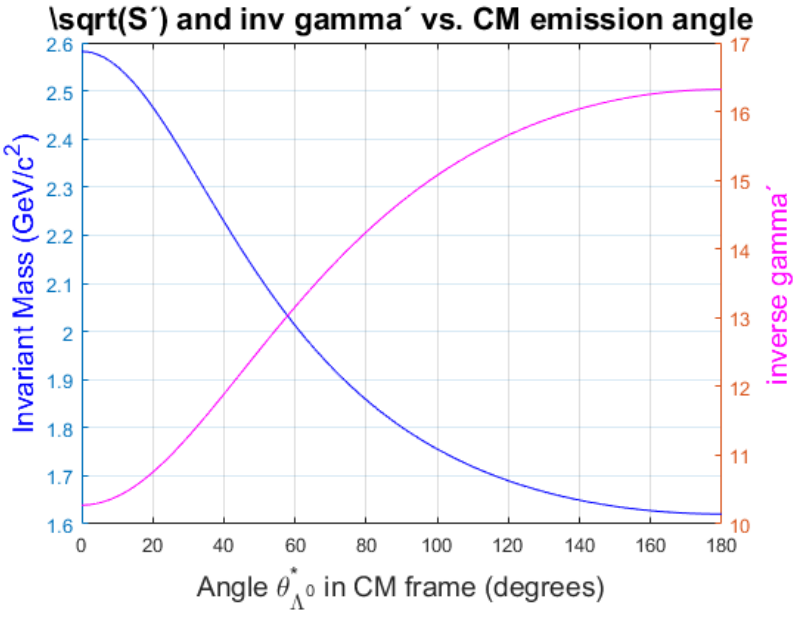

Figure 15: Invariant mass and Inverse gamma as a function of angle , = 20

Clearly, a lower inverse gamma factor leads to a higher invariant energy and a higher inverse gamma factor leads to lower invariant energy. The magnitude of the inverse gamma factor determines how close we reach to the rest frame of the system, therefore a low inverse factor results in a system that still moves a higher energy as compared to a high inverse factor. Combining this all, the magnitude of m translates into an energy distribution instead of a delta peak in the energy spectrum obtained when m = 0. Also, the magnitude of m influences the inverse Lorentz transformations through the variation of the inverse gamma factor and therefore it determines the *width* as well as the *position* of the distribution relative to the correct invariant mass of the parent particle. The minimum difference in reconstructed mass appeared to be 0.300 GeV/c^2, as shown by figure (13). Although not simulated, the boost factor from the CM to the Lab frame, and thus the energy of the parent particle in the lab will also contribute to the magnitude of the effect the m has in the reconstruction.

5 Decay Angular Distribution

In physics symmetries are important concepts and each symmetry has as a consequence a conservation law. Throughout the previous sections we have made use of this to relate the initial and final states of interactions. In particular for two-body decays, it has been shown when only applying two such symmetries, we were able to fully determine the kinematics of the process. So far, we only have considered the case in which none of the two product particles had a preferential direction of emission, leading to a uniform distribution of the emission spectrum. In section 3.2 we have been introduced to the amplitude M and the phase-space which proved to be key to a possible origin of anisotropy in the emission distribution. However, the nature of different interactions have not been discussed and neither their effects on a differential decay rate. For the purpose of further analysis we will discuss symmetries and their role in modification of the differential decay rate. This will be mostly done using a phenomenological approach and no qualitative derivations or expression will be shown.

5.1 Symmetries and Forces

Interactions or forces between elementary particles are mediated by force carriers or intermediate particles, each corresponding to a fundamental force. There are four such forces, namely: the electromagnetic, weak, strong and gravitational force, of which the first three are described by theories known as the Standard Model. Depending on their nature, particles experience one or multiple forces. The Standard Model is able to describe interactions with very high precision. In the field of particle physics, high energy experiments are designed to probe interactions at high accuracy to test the Standard Model and put constraints on new theories collectively referred to as beyond Standard Model (BSM), which aims for covering deficiencies of the Standard Model.
The character of each the individual forces upon a conservation laws is of interest. For this purpose symmetries can be subdivided in exact and approximate interaction symmetries. An approximate conservation law is recognizable if the interactions in which the law is violated are weaker than those in which it holds[11]. This can be illustrated by considering the law of parity conservation. Although the law is respected by gravitation, electromagnetic and strong interaction, it is violated by the weak interaction. This directly initiates the remaining part of the quest for a candidate process to incorporate an anisotropic decay distribution.

5.2 Parity Violation in Weak Interaction

Parity is known as the mirror-symmetry and utilizes the thought that the laws of nature are expected to remain unchanged when examined in a mirrored experiment. Until the beginning of the 1950s this seemingly obvious symmetry of nature held, until Lee and Yang questioned it in their paper '*on conservation of parity in weak interactions*'[12]. They suggestes an experiment involving beta decay, which shortly after was carried out by Wu[13]. Beta decay is the transformation of a neutron in a proton or vice versa, and is mediated by the weak interaction. The experiment used Cobalt-60, to study negative beta decay: $n \; ! \; p + e \; + \bar{}_e$. The following figure illustrates the effect of a parity transformation upon the expect electron emission:

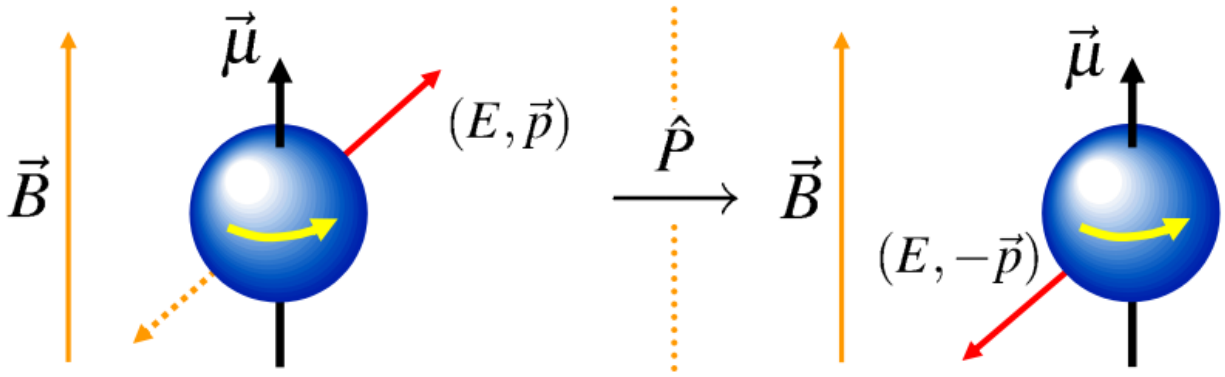

Figure 16: Parity transformation ; left the normal configuration, on the right the mirror image.

A parity transformation corresponds to inversion of the spatial coordinates. The spin is an axial vector, hence it remains unchanged under a parity transformation. If parity would be a true symmetry of nature one would expect no preferential emission in the (E, $\vec{p}$)- over (E, -$\vec{p}$)-direction, taken with respect to the axis of the spin of Cobalt-60. During the experiment the magnetic moment is oriented in the z-direction using a magnetic field. Flipping the magnetic field corresponds to alignment of the spin along the negative z-direction, allowing to measure the mirror configuration. If now an electron is emitted with in direction (E, -$\vec{p}$) with respect to orientation of the original spin alignment, one would expect the rate to be equally likely to emission in the (E, $\vec{p}$) direction.

The experiment showed that the electrons favored an emission angle opposite to the spin , establishing parity violation. In fact, later this was determined to be maximal. It is a well known experiment in the field of particle physics and serves as a perfect example of an anisotropic distribution. The weak interaction interacts only with left-handed chiral components of particles and right-handed chiral components of anti-particles, therefore the mirror image corresponding to right-handed particles is highly suppressed. Left- or right-handed refers to the orientation of the spin with respect to a particles momentum. The spin is aligned in the direction of the momentum in the case of right-handed, left corresponds to opposite configuration and hence, it is a frame dependent quantity.

5.3 Anisotropy in Hadronic Decay

The previous paragraph illustrated several important aspects to be taken into account in the pursuance of the main objective of this thesis. The Wu-experiment shows that one needs to align the particle in order to measure the angular distribution. Hence, a possible candidate is force to have intrinsic spin, not only for the purpose of measuring the distribution, but also for the ability to orientate the distribution to something in the first place. Thus, to obtain an analytic expression for such a total decay rate a scalar theory and averaging over the spin states is not sufficient if one wants do derive it. The importance of polarization and alignment for determining the spins of particles is that unstable particles which are unpolarized and unaligned decay isotropically[11].

Besides beta decay, hyperons and mesons where also put forward for candidate experiments to provide evidence for parity conservation or non-conservation. This interest for the fact that semi-leptonic decay must be disregarded when restricting to a two-body decay. Turning our attention to mesons and hyperons decays, with special attention to weak decays. It is found that for the specific case of a particle decay to a spin $\frac{1}{2}$ particle and a spin 0 particle, the parity cannot be determined without a measurement of the polarization of the final spin $\frac{1}{2}$. Moreover, if a particle decays into a spin 0 and a spin $\frac{1}{2}$ particle with non-conservation of parity and has a angular emission probability, with is taken with respect to the z-axis:

$$W( )d \quad / \ (1 + \quad \cos \ )d \ ; \tag{52}$$

then the magnitude of may give information about the spin of the decaying particle[11] and it depends on the weak decay mechanism. Only a numerical evaluation leads to a useful result for expressing $W(\ )$[14]. Since it shows a complicated dependence on the kinematics and energies of the system. Measuring an angular emission distribution can be used as a method of applying spectroscopy on the unstable particle. Also, note that no azimuthal angle appears in this distribution, corresponding to cylindrical symmetry around the spin axis. There are some theorems that apply for methods of obtaining information on either spins or parities of particles. We will list two of them, firstly the highest power of cos which can occur in $W(\ )$ is $\cos^{2J}$, where J is the spin of the particle (Yang 1948). Secondly, if parity is conserved, only even powers of cos contained in $W(\ )$, when averaged over . For equation (52), Lee and Yang derived that is restricted to the following range, depending on J:

$$\frac{1}{6J} \quad \frac{}{3} \quad \frac{1}{6J}: \tag{53}$$

In the remainder of this paragraph we spend time on a decay that meets all the final criteria:

1. *Two-Body Decay*
2. *Possibility for misidentification*
3. *Weak decay*
4. *Non-zero spin unstable particle*
5. *Decay products are spin 0 and spin* $\frac{1}{2}$
6. *Alignment/Polarization*

As we have already seen, a possible decay process is:

$$\Xi \quad ! \ \Lambda^0 + \tag{54}$$

So far, we have only mentioned the weak force, which is a mediator between two elementary particles. It is not included in the kinematics of the process, we can however depict the process using the corresponding feynman diagram:

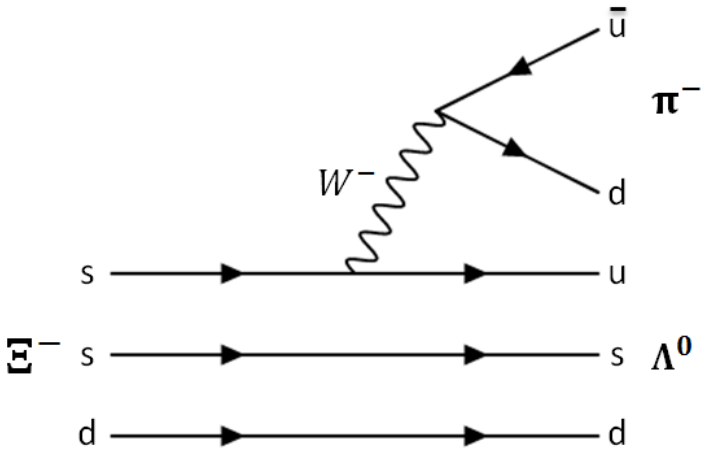

Figure 17: Feynman diagram for $\Xi \quad ! \ \Lambda^0 +$

Parity is not conserved in the decay of Ξ . For this reaction the measured value of the asymmetry parameter in its decay is[11]

$$= +0{:}47 \quad 0{:}16{:} \tag{55}$$

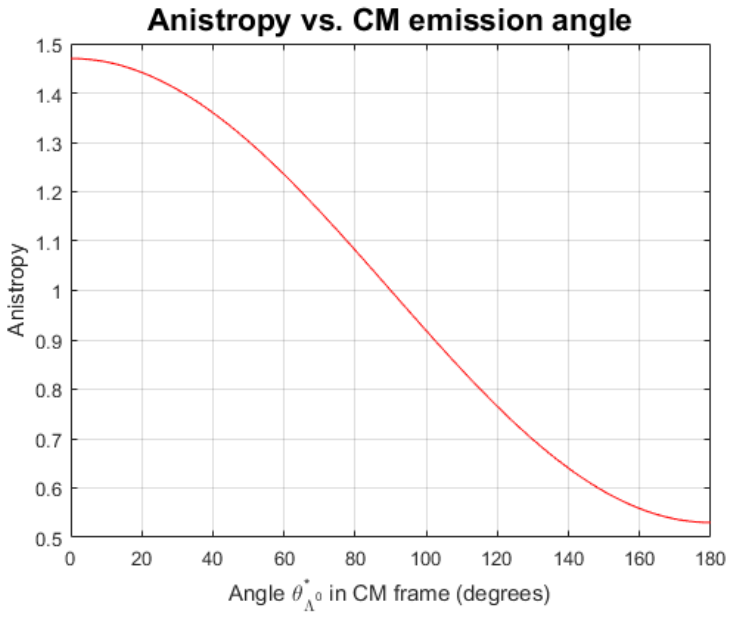

Figure 18: Relative emission distribution as a function of

The relative anisotropy in emission graphically shown, corresponds to 1.47 in forward direction and 0.53 backward direction. This parameter is associated with the lambda, which in fact was the reason for choosing as reference in the emission distribution instead of referring to the particle of misidentification. Since the pion is spinless is does not feel suppression in any direction. However, due the kinematic constraints in a two-body decay in the center-of-mass system we know that the emission is back-to-back. Hence, the pion is coupled through this kinematic constraint and the resulting emission distribution is opposite to that of the lambda. This is of importance for the fact that we substitute the pion for a kaon, resulting in different energies but 'filtered' in equally manner. To illustrate its angular emission distribution, we use figure (9) from the previous section on a two body decay. This illustration shows the angular distribution of the lambda in both the CM and Lab frame. It is here that we have to make the assumption that the spin of the cascade is *polarized* along the z-axis in its direction of motion.

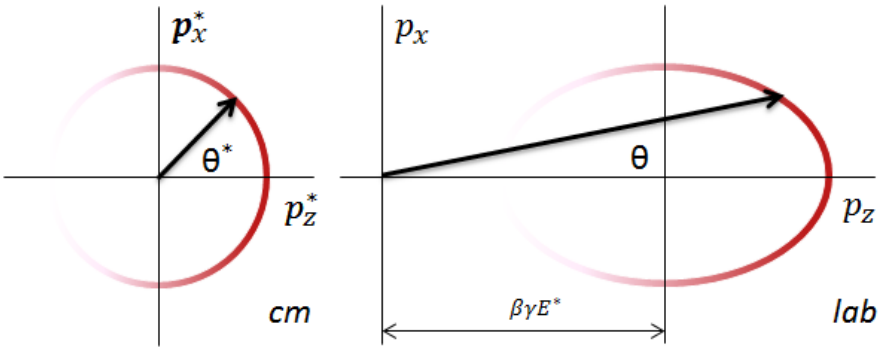

Figure 19: Lorentz transformation of an anisotropic -distribution

The intensity of the circle displays the probability to decay at an angle , the width of the line is thicker than the one in figure (9) to illustrate the total amount of particles remains unchanged. The decay product has a preference to decay in the forward z-direction. One may conclude, that for a large parameter , one of the two solutions for may be neglected, since there is almost no contribution left. Lets have a look of what the signature of the histogram now looks like when applying this emission distribution on the reconstruction of the 'invariant' CM energy in the case of a misidentification.

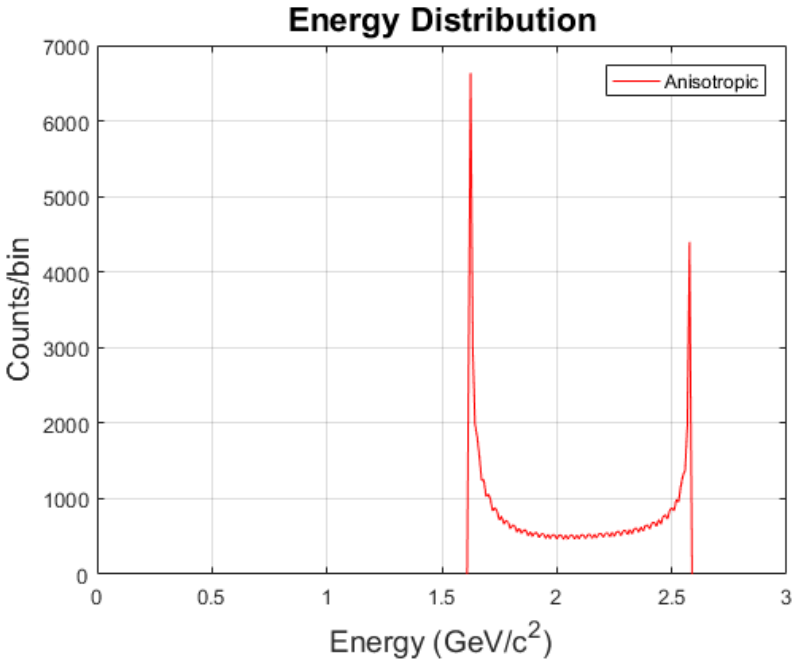

Figure 20: Anistropic distribution E = 0.01 GeV/c^2, N = 100000

Evidently the spectrum shifter towards the high energy, correspond to the forward direction of emission. The number of particles emitted in this distribution is equal to the previous, isotropic case. For clarity of the effect of such an anisotropic function on the distribution, both graphs are depicted in the figure (21). The low end peak is cut in half and the number of particles emitted with higher energy has increased. Only the signature of the distribution has changed, both the position and the width of the reconstructed CM energy remain unchanged under the effect of an anisotropic emission distribution.

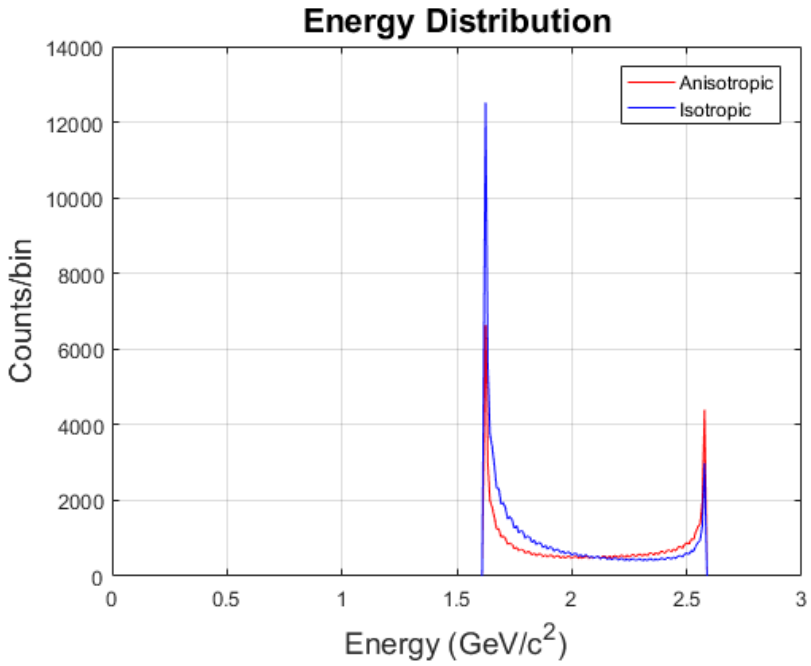

Figure 21: Anisotropic and Isotropic distributions

Together with the concluding section of paragraph 4.4, most effects of an anisotropic emission distribution in case of - K misindentification of the cascade decay have been discussed. To conclude, we represent the graph which contains all derived energy spectra and therefore reflects the final result of this thesis.

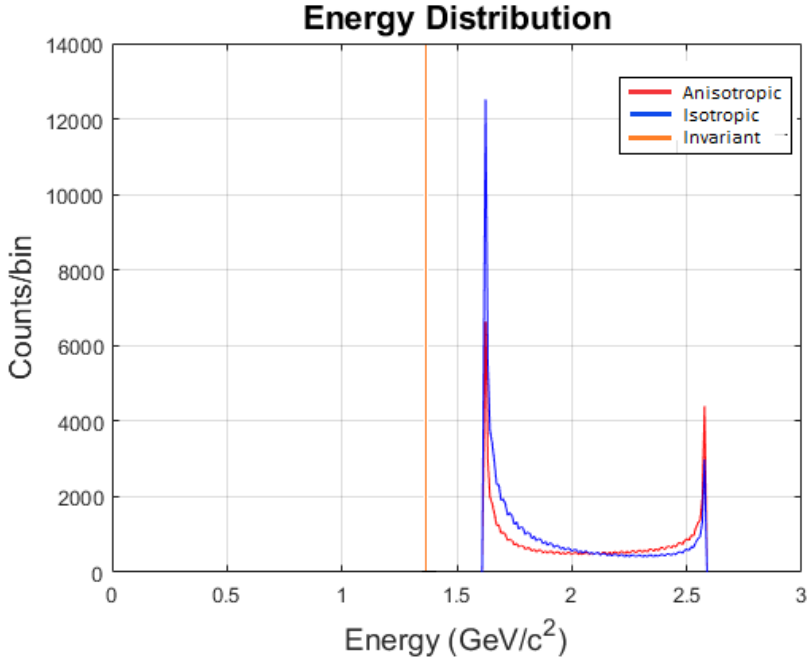

Figure 22: Invariant energy, Anisotropic and Isotropic distributions

6 Discussion

The development throughout the sections have presented some of the fundamental properties which are needed to be taken into account for the derivation of angular emission distribution. Reflecting on the encountered material, two major attitudes towards the underlying objective of this thesis might be taken.

The first regarding purely the intention of exploring the origin of an anisotropic distribution. It has proved to be of complex nature and although, qualitatively a lot has been discussed, the physics involved in a single derivation is rather complex. In order to perform the calculations one needs to be acquainted with field theories on a high level. The modification of the differential decay rate such that it results in a higher probability in a given space direction is not straightforward. The weak interaction proved to be a candidate for this, since it violates the law of parity violation.

For a proper identification of the secondary particles, reconstruction ends up at the correct energy of the cascade particle. Since reconstruction over all emission angles of lambda in the CM frame are correctly performed to obtain the same invariant energy, anisotropy has no influence on the obtained invariant energy spectrum. In case of a single misidentification, reconstruction of the invariant energy leads to a distribution. For this the obtained anisotropic emission distribution together with the kinematics of a two-body decay leads to a shift towards to high energy side of the energy distribution. For further study it is of interest to insert the additional mass in a system boosted to a different energy in the lab frame and then examine if the width changes proportionally as well as the position of the reconstructed energy spectrum.

Secondly, the necessity of taking such detailed information into account for the purpose of improving event reconstruction in experiments. Principally, alignment and polarization have shown to be the main conditions for obtaining information on the distribution. Therefore, if a distribution is anisotropic one could raise questions on whether these conditions apply and cause such deviation that it needs to be considered. Also, lifetimes associated with weak decaying particles are of the order of 10 ^{10}s. The lifetime together with a -factor of 20 leads to a decay length for the cascade to be around 60 centimeters, which is most likely enough for a detector to identify it. Hence, for the weak interaction, identification through an anisotropic distribution will not be as necessary as for exotic short lived particles. The examination of anisotropy due to the strong interaction is of interest for further study.

7 Conclusion

This thesis has elaborately treated two-body decays and their dependence on underlying physical principles. It has been successfully pointing out the main aspects of a two-body decay and its corresponding distribution. In case of a boost of a -factor of 20, the invariant energy reconstruction of a two-body decay has been treated in the case of both a proper identification and a single misidentification. Additionally the effect of an anisotropic emission distribution due to the weak interaction has been studied. The results have shown that in case of correct identification the angle of emission in the center-of-mass system does not effect the reconstructed energy, hence resulting in an invariant energy spectrum. Since there is no angular dependence, adding an anistropic emission distribution does not affect the invariant energy spectrum. For a single misidentification, the reconstructed 'invariant' energy is in fact not invariant and corresponds to a distribution depending on the emission angle in the center-of-mass frame. The amount of misidentified mass determines the width as well as the position of the energy distribution relative to the correctly identified invariant mass. The effect of additional mass on the distribution is influenced by the magnitude of the boost applied to the center-of-mass system. The anisotropic emission distribution only influences the obtained invariant energy spectrum by changing the intensity from one end to the other end.

8 Acknowledgements

Although most hours are spend individually throughout the course of the project, the weekly discussions with fellow members of the LHCb group gave me a good sense of collective effort. The support of Jim Baarslag has been truly appreciated. Especially, I am grateful to my supervisor, Gerco Onderwater, for his guidance, the discussions we have had and for introducing me to the exciting world of particle physics.

A Appendix

A.1 Special Relativity

The *Special Theory of Relativity* forms part of the fundamentals of modern physics. It is a generally accepted and experimentally well confirmed theory based on two postulates:

1. *The Principle of Relativity*

   The laws of physics are the same in all inertial frames of reference.

2. *The Constancy of Speed of Light in Vacuum*

   The speed of light has the same value c in all inertial frames of reference.

This section will be used to study the profound consequences these postulates have for the connection between space and time. A brief introduction in Lorentz transformations will be given first, followed by the vector notation commonly used in high energy physics. Finally, one uses conservation laws in order to derive constraints of a specified type of reaction.

A.2 Lorentz Transformations

According to the *Special Theory of Relativity*, the laws of physics are equally valid in all *inertial* reference systems. An inertial reference frame is defined to be a system moving with a constant velocity, i.e. a non accelerating frame. Now define a point in space-time by its coordinates t, x, y, z in a frame S. Consider a second intertial-frame S', moving with a constant velocity with respect to the z axis of frame S. is defined as $\frac{v}{c}$, using natural units ($c = 1$), $v =$ directly follows. This is shown in figure 23.

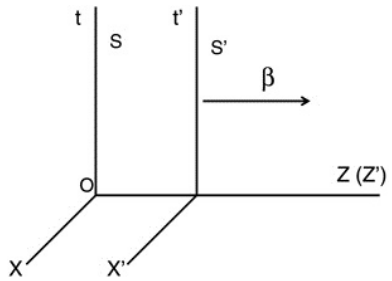

Figure 23: Inertial frame S' moving with velocity with respect to the z-axis of inertial frame S

If one wants to obtain this point in frame S', the relationship between coordinates in S and S' is needed. This relation follows from the theory of special relativity and goes under the name *Lorentz transformation*. A Lorentz transformation describes how coordinates in different inertial frames are linked by considering the *relative* velocity between the two frames. To obtain the coordinates t', x', y' and 'z in frame S' one use the following Lorentz transformation

$$\begin{aligned} t' &= (t \quad z) \\ x' &= x \\ y' &= y \\ z' &= (z \quad t) \end{aligned} \tag{56}$$

where

$$= \frac{1}{\sqrt{1 \quad ^2}} \tag{57}$$

is the Lorentz factor. The inverse Lorentz transformation is given by interchanging the apostrophes and replacing the minus signs by pluses. This type of Lorentz transformation is called a *boost*, a rotation in which the temporal and spatial part rotate in opposite direction. In the next section we well derive a boost fully and also deduce the Lorentz factor. From Lorentz transformations one can derive a number of consequences;

1. *The relativity of simultaneity*
   $t_a = t_b \quad \textit{and} \quad t'_a = t'_b + \frac{v}{c^2}(x_b \quad x_a)$
2. *Lorentz contraction*

   A moving object is shortened by a factor along the direction of motion

3. *Time dilation*

   Moving clocks run slow t = t'

4. *Velocity addition*
   $u = \frac{u' + v}{1 + \frac{u'v}{c^2}}$

This is the natural output of the two fundamental postulates of the special theory of relativity. A slight touch upon these consequences is made several times throughout the next sections. As we already have quietly extended our three dimensional physical reality to a four dimensional space-time, known as Minskowski space. It is now time to develop the associated notation used when working in the relativistic regime.

A.3 Four vectors

In high energy physics the notion of absolute time is no longer valid. Typical colliders are of such energy that one has to expand the view of classical three dimensional world to a modern world in which time is on equal footage to space. That is to say there are three spatial dimensions and one temporal. In order to do calcutations in particle collisions, it is convenient to use a proper notation. At the end of this section the behaviour of the temporal and spatial part of a space-time vector is further examined.

Four-vector or position-time four-vector is the natural extension of euclidean vector, which consists of dimensions x, y and z. Along with the extra dimension, the index notation together with the so called Einstein summation convention are widely used in the relativistic regime of physics. A four-vector is of the form:

$$x \ ; \qquad = 0; 1; 2; 3 \tag{58}$$

where is the index and the components of the vector are:

$$\begin{aligned} x^0 &= ct \\ x^1 &= x \\ x^2 &= y \\ x^3 &= z \end{aligned} \tag{59}$$

In particular interest are the combination of coordinates which remain unchanged under specific transformation, these are invariant properties. An euclidean vector has a combination of coordinates $r^2 = x^2 + y^2 z^2$ that is invariant under rotations. This norm r^2 is known as the dot-product of two three-vectors, calculated as follows:

$$r^2 = \sum_{=1} x \; x \tag{60}$$

In order to find such a combination for a four-vector we need to find a way to extend the euclidean form to space-time. The following property I is invariant under the four dimensional equivalence of a rotation, the previously introduced Lorentz transformations:

$$I = (x^o)^2 \quad (x^1)^2 \quad (x^2)^2 \quad (x^3)^2 \tag{61}$$

One directly notices the minus signs. To include these a metric tensor g_{uv} is introduced:

$$g = \begin{pmatrix} 1 & 0 & 0 & 0 \\ 0 & 1 & 0 & 0 \\ 0 & 0 & 1 & 0 \\ 0 & 0 & 0 & 1 \end{pmatrix} \tag{62}$$

$$g = g^{\;1} \quad \textit{and} \quad g_{00} = 1; \quad g_{ii} = \quad 1$$

Where greek letters are used as indices of the metric g and the i's to denote entries of the spatial part of the metric. One can now write down I in a compact fashion:

$$I = \sum_{=0 \;\; =0} g \quad x \; x \tag{63}$$

The 'original' four vector with index up can be transformed into one carrying the index down. The transformation of a contravariant vector into a covariant vector using the metric is done in the following manner:

$$x_u \quad g \quad x$$

i.e.

$$x_0 = x^0; \quad x_1 = \quad x^1; \quad x_2 = \quad x^2; \quad x_3 = \quad x^3$$

adding this, the invariant property I can be written in it's purest form, using summation convention:

$$I = x \; x \tag{64}$$

A.4 Energy and Momentum

With the previous two sections in mind we can turn our focus on combining the two and gain some results. If we take a closer look at time dilation, the amount of time passed on in internal clock of a particle moving at velocity v, is what's known as the the particles proper time. It related to the time measured by a clock at rest as follows:

$$d \quad = \frac{dt}{} \tag{65}$$

where is again the Lorentz factor, depending on the particles velocity. The time measured in a frame at rest is 'dilated'. A beautiful illustration of this are the cosmic muons. The expected muon flux would be only a small fraction of what is observed on earth when not taking relativistic effects into account on a particles lifetime. Therefore, it serves as a well accessible example of the importance of time dilation. A precise experiment on the differences between expected and observed muon flux was measured in Frisch-Smith experiment conducted in 1963.

Now similar, we can consider velocity in the lab frame:

$$v = \frac{d\vec{x}}{dt} \tag{66}$$

and in the particles rest frame:

$$\frac{d\vec{x}}{d} \tag{67}$$

which is called proper velocity. Again the lorentz factor relates the two; = v. Now using explicit index notation, let's have a look at the 'proper' derivates.

$$\begin{aligned} &= \frac{dx}{d} \\ {}^{0} &= \frac{dx^0}{d} = \frac{ct}{dt} = \quad c \\ {}^{i} &= \frac{dx}{d} = \quad v_i \end{aligned}$$

Resulting in

$$= \quad (c; v_x; v_y; v_z) \tag{68}$$

and

$$= \quad {}^2(c^2; v_x^2; v_y^2; v_z^2) = \quad {}^2c^2(1 \quad \frac{v^2}{c^2}) = c^2 \tag{69}$$

which is manifestly invariant.

Time has now come to expand this to momentum to finally look at what invariant quantity can be obtained, since it will be shown that this property is of special interest in detectors. We start defining momentum, by including mass in the previous given definition of proper velocity:

$$p \quad m \tag{70}$$

again we can write this as a four vector:

$$p \quad = m \tag{71}$$

Using the proper derivatives the temporal and spatial components can be obtained:

$$p^0 = \quad mc \tag{72}$$

$$\mathbf{p} = \quad mv = \frac{mv}{1 \quad \frac{v^2}{c^2}} \tag{73}$$

If we define relativistic energy E as $E = \ mc^2$ the first temporal component of the momentum four vector can be written as:

$$E \qquad mc^2 = \frac{mc^2}{\frac{v^2}{c^2}} \tag{74}$$

And so the zeroth component of p is then $\frac{E}{c}$. This is the final ingredient in developing the energy-momentum four-vector. Which appears as follows:

$$p \ = (\frac{E}{c}; p_x; p_y; p_z) \tag{75}$$

As expected, now the computation of the 'inner product' follows.

$$p \ p \ = \frac{E^2}{c^2} \quad p^2 = m^2c^2 \tag{76}$$

Finally we have derived ourselves one of the most famous equations of relativistic theory, namely the invariance of mass. Using natural units:

$$\boxed{m^2 = E^2 \quad \mathbf{p^2}}$$

The energy momentum four-vector can be given in the following notation with the corresponding components:

$$P \ ; \qquad = 0; 1; 2; 3 \tag{77}$$

$$\begin{aligned} P^0 &= E \\ P^1 &= p_x \\ P^2 &= P_y \\ P^3 &= P_z: \end{aligned} \tag{78}$$

A.5 Rapidity

The LHCb is a single arm detector designed such that it covers a relatively small opening angle with respect to the beam axis to cover high -factors. Previous sections have shown the effect of a boost on a arbitrary two body decay. The momentum of the daughter particles increases in the direction of flight of the decaying particle. High -factors are common at the LCHb, resulting in a trajectory close to the beam axis. Two close related variables shown te be usefull in detectors physics will be introduced in this section. Although they are not invariant themselves, properties derived from them are independent of boosts to an observers rest frame. The springboard is the consideration of particle with mass M and it's energy-momentum-mass relation.

$$E^2 = p_x^2c^2 + p_y^2c^2 + p_z^2c^2 + M^2c^4 \tag{79}$$

If we now consider a Lorentz boost with respect to the z axis using the corresponding Lorentz transformation, we can differentiate between components which either are or aren't affected by the boost. The x and y components of the particle's momentum are perpendicular to the direction of the boost and together with it's mass these form the invariant quantities. We gather them and define this as the transverse mass M_T.

$$M_T^2c^4 = p_x^2c^2 + p_y^2c^2 + M^2c^4 \tag{80}$$

In an accelerator the particles colliding do not always have equal and oppposite momentum. Therefore, the centre of mass frame does not correspond to the lab frame and has a velocity with respect to the z-axis. In addition to transverse mass we can also define a quantity called rapidity:

$$y = \frac{1}{2}\ln\frac{E + p_zc}{E \quad p_zc} \tag{81}$$

Now consider a highly relativistic collision, depending on direction of the products there are two extreme values. Consider a particle directed in the xy-plane, the p_z will be low and the corresponding value of y will tend to be 0. When it is predominantly directed along the beam axis, p_z is either in the plus or minus direction. As E ' p_zc in at high energies, y will be either $+1$ or $\quad 1$. So, the rapidity is 0 when particle is travelling transverse to the beam axis and tends to $\quad 1$ when it is close to the beam axis. The precious formula can be rewritten:

$$y = \ln\frac{E + p_z}{M_Tc^2} \tag{82}$$

Although one can clearly see the dependence of this quantity upon the specific frame of reference. Differences between rapidity's of two particles is an invariant property. This is why they are of special interest in accelerator physics. Together with the azimuthal emission angle , the particle can be given a coordinate pair (y,). Both differences in rapidity as well as the emission angle are invariant with respect to Lorentz boosts.

Histograms consisting of either angular separation or rapidity separation can be contributed by events with an arbitrary velocity with respect to the detector frame.

A.6 Pseudo-rapidity

However, for highly relativistic particles it can be hard to measure both momentum and energy. Especially at high rapidities the beam pipe may be in the way of measuring the quantities properly. What follows next is the definition of another quantity closely related to rapidity, which is easier to measure and turns out to be very similar to rapidity for highly energetic particles. We start by using the previously introduced definition of rapidity:

$$
\begin{aligned}
y &= \frac{1}{2}\ln\frac{E + p_z c}{E \quad p_z c} \\
&= \frac{1}{2}\ln\frac{(p^2c^2 + m^2c^4)^{\frac{1}{2}} + p_z c}{(p^2c^2 + m^2c^4)^{\frac{1}{2}} \quad p_z c}
\end{aligned}
\tag{83}
$$

For a highly relativistic particle, pc is dominant over mc^2. With the use of a binomial expansion we can approximate the above equation.

$$
\begin{aligned}
y &= \frac{1}{2} ln \frac{pc(1 + \frac{m^2c^4}{p^2c^2})^{\frac{1}{2}} + p_z c}{pc(1 + \frac{m^2c^4}{p^2c^2})^{\frac{1}{2}} \quad p_z c} \\
&\text{'} \frac{1}{2}\ln\frac{pc + p_z c + \frac{m^2c^4}{2pc} + :::}{pc \quad p_z c + \frac{m^2c^4}{2pc} + :::} \\
&\text{'} \frac{1}{2}\ln\frac{1 + \frac{p_z}{p} + \frac{m^2c^4}{2p^2c^2} + :::}{1 \quad \frac{p_z}{p} + \frac{m^2c^4}{2p^2c^2} + :::}
\end{aligned}
\tag{84}
$$

Now, using $\frac{p_z}{p} = \cos(\ )$, where is the angle made by the trajectory of the particle with the z-axis. Using this relation we can rewrite the above equations:

$$
\begin{aligned}
1 + \frac{p_z}{p} &= 1 + cos \ = 1 + (cos^2\frac{}{2} \quad sin^2\frac{}{2}) = 2cos^2\frac{}{2} \\
1 \quad \frac{p_z}{p} &= 1 \quad cos \ = 1 \quad (cos^2\frac{}{2} \quad sin^2\frac{}{2}) = 2sin^2\frac{}{2}
\end{aligned}
\tag{85}
$$

Substituting these back into (83) we obtain:

$$
y \text{ ' } \frac{1}{2}\ln\frac{cos^2\frac{}{2}}{sin^2\frac{}{2}} = \quad \ln\tan\frac{}{2} \tag{86}
$$

We can now define pseudo-rapidity as

$$
= \quad \ln\tan\frac{}{2} \tag{87}
$$

along with a graphical representation of the common used absolute value.

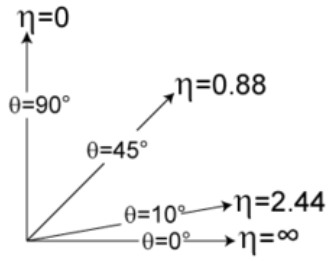

Figure 24: Pseudorapidity

Source: wikipedia.org

For highly relativistic particles 1 and so y' . Pseudo-rapidity is used in hadron colliders, since the center of mass frame often does not coincide with the detector frame. In contrast to rapidity, pseudo-rapidity does not have the involvement of physics and therefore it is an easier to determine quantity. The fact that at high energies the two become almost identical results in a preference of over y.

References

[1] Christian Lippmann. Particle identification. *Nuclear Instruments and Methods in Physics Research Section A: Accelerators, Spectrometers, Detectors and Associated Equipment*, 666:148–172, 2012.

[2] Gideon Dror, Halina Abramowicz, and David Horn. Vertex identification in high energy physics experiments. In *Advances in Neural Information Processing Systems*, pages 868–874, 1999.

[3] Roel Aaij, A Affolder, K Akiba, M Alexander, S Ali, RB Appleby, M Artuso, A Bates, A Bay, O Behrendt, et al. Performance of the LHCb vertex locator. *Journal of Instrumentation*, 9(09):P09007, 2014.

[4] Brian R Martin. *Nuclear and particle physics: an introduction*. John Wiley & Sons, 2006.

[5] A Augusto Alves Jr, LM Andrade Filho, AF Barbosa, I Bediaga, G Cernicchiaro, G Guerrer, HP Lima Jr, AA Machado, J Magnin, F Marujo, et al. The LHCb detector at the LHC. *Journal of instrumentation*, 3(08):S08005, 2008.

[6] M Adinolfi, G Aglieri Rinella, E Albrecht, T Bellunato, S Benson, T Blake, C Blanks, S Brisbane, NH Brook, M Calvi, et al. Performance of the LHCb RICH detector at the LHC. *The European Physical Journal C*, 73(5):2431, 2013.

[7] Vitaliĭ Iosifovich Goldanskiĭ and Iosif Leonidovich Rozental. *Kinematic methods in high-energy physics*. CRC Press, 1989.

[8] David Griffiths. Introduction to elementary particles, 2004. Technical report, ISBN 0-471-60386-4.

[9] LD Landau and EM Lifshitz. Fluid Mechanics, Pergamon. *New York*, 61, 1959.

[10] Lev Davidovich Landau and Evgenii Mikhailovich Lifshitz. *Quantum mechanics: non-relativistic theory*, volume 3. Elsevier, 2013.

[11] D Lichtenberg. Meson and baryon spectroscopy. *Ergebnisse der exakten Naturwissenschaften*, 1965.

[12] Tsung-Dao Lee and Chen-Ning Yang. Question of parity conservation in weak interactions. *Physical Review*, 104(1):254, 1956.

[13] Chien-Shiung Wu, Ernest Ambler, RW Hayward, DD Hoppes, and R Pl Hudson. Experimental test of parity conservation in beta decay. *Physical review*, 105(4):1413, 1957.

[14] Keijo Kajantie and E Byckling. *Particle kinematics*. Wiley-Interscience, 1973.